Analysis of Electrically Large Patch Phased Arrays via CFDTD

Thinh Q. Ho*, Lilton N. Hunt, Charles A. Hewett
SSCSD 282, San Diego, CA 92152
Thomas G. Ready
NAVSEA PMS 500, Washington, DC 20376

Raj Mittra, Wenhua Yu
RMA, State College, PA 16803
Dale A. Zolnick, Mark Kragalott
NRL 5314, Washington, DC 20375

I. Introduction

The design complexity of phased array antenna systems has resulted in an increased need for accurate methods to predict performance. Reliable CEM tools and computing power can reduce development costs and time. A newly developed Conformal Finite Difference Time Domain (CFDTD) code [1,2] is utilized to rigorously model and analyze a 10,000-element rectangular patch phased array at L-band. In order to run such a numerically large antenna structure the code was parallelized and executed on a 64-bit, 26 dual processor node computer cluster. CFDTD is a general solver capable of accurately analyzing a wide variety of radiators. Parallel processing and a highly versatile non-uniform meshing capability are two aspects of CFDTD that ease otherwise restrictive computational resource demands. In large array designs, various methods based on infinite array via periodic boundary conditions are frequently used. However, these techniques do not account for the edge effects due to the radiating elements located at the boundary of the actual finite array structure. In addition, the mutual impedance is only valid from the infinite array perspective. Verification and validation was conducted on a smaller array to ensure accuracy prior to scaling up to the full size array. Antenna radiation patterns and directivity values are presented as a function of scan angle along with computational details.

II. Array Design

The geometry of the patch array with radiating elements spaced 0.5λ apart is shown in Figure 1. The spacing is defined as the separation distance between two adjacent feed points. The physical dimensions of the patches are 5.00 cm x 4.17 cm. The supporting substrate is 0.36 cm thick with a dielectric constant of 2.64. The elements are arranged in a square lattice with an overall array size of 885.46 cm x 886.33 cm ($2500\lambda^2$). Each element is excited at the center of the short edge by placing an electric field at the gap between the ground plane and the probe feeding the patch. The model is constructed as a single finite antenna structure, with a back-plate serving as an RF ground. Non-uniform meshing is applied with a finer discretization in the vicinity of the feed and a coarse grid elsewhere in order to make the model computationally efficient in terms of RAM. The model used perfectly matched layer boundary conditions to truncate the computational domain. The large, flat nature of planar phased arrays leads to an elongated computational domain, which makes avoidance of obliquely incident waves difficult. These are waves that reflect off the terminations of the absorbing boundaries and enter back into the problem space corrupting the solution. The PML needs to be placed sufficiently far away from the radiating elements so that incoming waves are nearly planar and not very oblique. This requires an expansion of the problem space. In this array, all 10,000 elements are excited; therefore, a huge domain is required to prevent the partial reflection of oblique waves. The computational domain is divided equally among the 52 processors, with one-dimensional partitioning along the x-axis. This particular model required 25 GB of memory. The array was excited with a Gaussian pulse modulated by the center frequency of the operational band and was run for 70,000 time steps to ensure solution convergence. A uniform amplitude distribution across the array was implemented. Beam steering to 30°, 45°, and 60° away from boresight was accomplished by adjusting the time delay between radiating elements.

III. Results and Discussion

To validate the CFDTD code, analysis was first carried out on a smaller array with 64 elements. The structure was built up with elements identical to those used in the 10,000-element array. Models of the validation array were constructed using both CFDTD and XFDTD [3]. Figure 2 shows the array radiation patterns for 0°, 30°, 45°, and 60° scan angles at the center frequency of 1.75 GHz. The beam was scanned in the $\phi = 90°$ plane. The solid lines represent CFDTD data while the dotted lines indicate the corresponding XFDTD set. As the beam is steered away from boresight, the 3-dB beamwidth increases from 12.9° at boresight to 26.2° at the 60° scan angle. The first sidelobe level is about 13 dB below the peak when the main beam is pointed at boresight. The total change in peak sidelobe level is 4.0 dB as the beam is scanned from boresight to 60°. The array directivity calculated with CFDTD is 23.0 dB, which is within 0.2 dB of the value given by XFDTD. Furthermore, the scan loss from 0° to 60° is observed to be 3.0 dB with CFDTD and 2.8 dB with XFDTD. These values are consistent with expectations for a well behaved array with 0.5λ element spacing.

Using the previously described element, with the same lattice configuration, the physical surface array area is now more than 160 times larger. The height of the computational domain is five times larger to help reduce the incidence angle of waves impinging on the absorbing boundaries. A non-uniform meshing scheme, identical to the one employed in the 64-element validation case, was utilized throughout the calculation process for all scan angle models in order to maintain the accuracy. The 10,000-element case was spread across 52 processors. This case required a runtime of 36 hours per scan angle, compared with 1.25 hrs for the smaller array. The antenna performance for the large array is shown in Figure 3 at 0°, 30°, and 60° scan angles. The patterns are plotted in rectangular coordinates with an angular 60° window in order to show details in the main beam vicinity. The radiation pattern exhibits a well defined pencil beam due to its very large aperture size. The 3-dB beamwidth increases from 1.04° to 2.14° as the beam scans from 0° to 60°. In this design, we observe no grating lobes within the scan volume, even when the beam is scanned to 60°. The level of the first sidelobe pair does not dramatically change when the beam is scanned away from boresight as it did for the 64-element array. The back-lobe level is below 30 dB. Table 1 gives the directivity values at different scan angles. The directivity edges slightly higher, from 44.46 dB to 44.73 dB, across the 100 MHz band. A directivity of 44.65 dB is computed at the center frequency of 1.75 GHz. Furthermore, the calculated scan loss between 0° and 60° is about 3.15 dB.

Acknowledgements

This work was funded by NAVSEA PMS 500, under the Integrated Topside Design VIPER program. The authors thank Michelle Bui from SSCSD for her contributions to the development of the computer clusters.

References

[1] W. Yu and R. Mittra, *Conformal Finite Difference Time Domain Solver*, New York: Artech House, 2004.

[2] T. Q. Ho, C. A. Hewett, L. N. Hunt, T. G. Ready, and R. Mittra, "Lattice Spacing Effect on Scan Loss for Bat-Wing Phased Array Antennas", 2005 IEEE/ACES International Conference on Wireless Communications and Applied Computational Electromagnetics Proceedings.

[3] REMCOM, "XFDTD version 6.2" dated 2004.

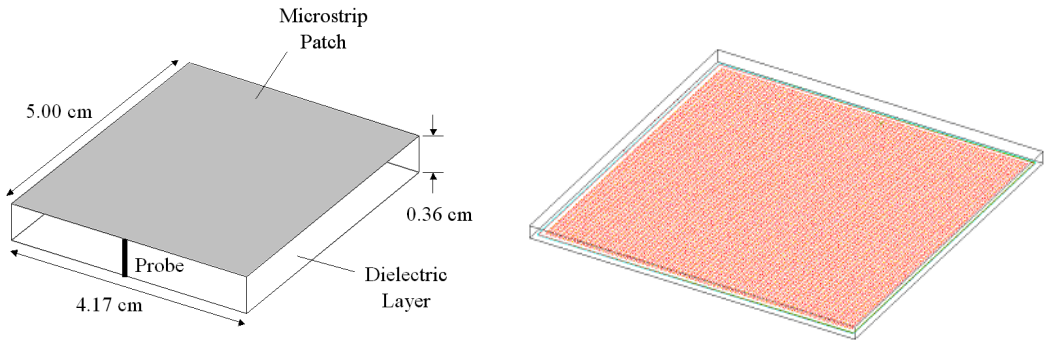

Figure 1. 10,000-element rectangular patch antenna array.

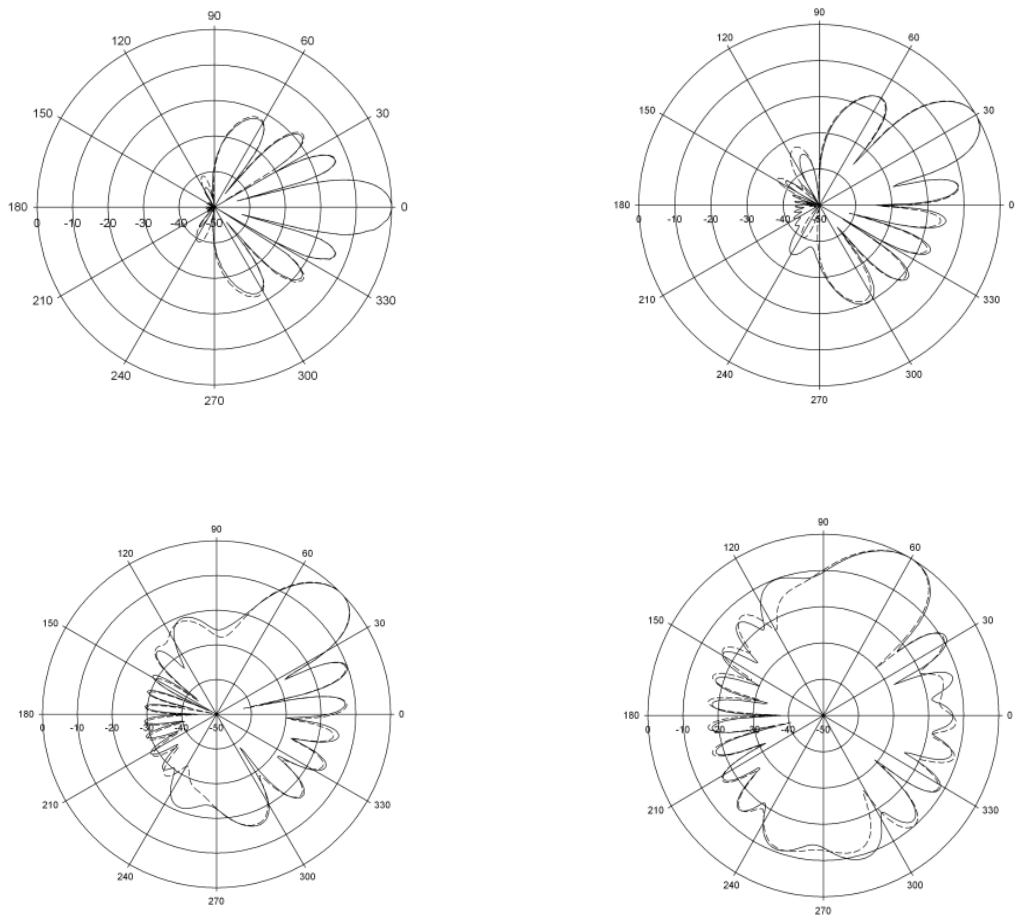

Figure 2. Radiation patterns at scan angles of 0°, 30°, 45°, and 60° from a 64-element design.

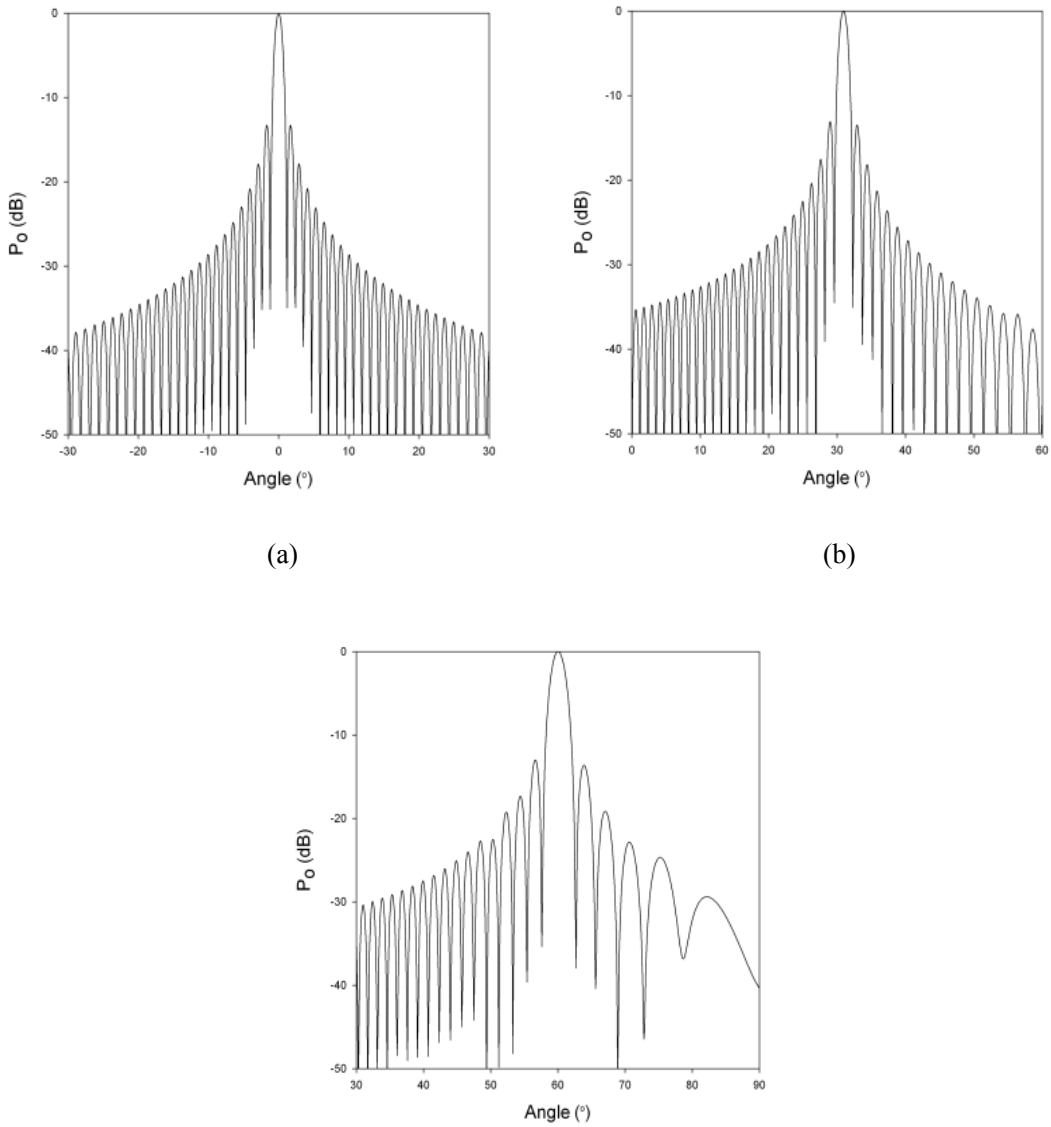

Figure 3. Radiation patterns of the 10,000-element patch L-band array with 0.5λ spacing. Scan angle (a) 0° (b) 30° (c) 60°.

Directivity 10K Elements (dB)			
Frequency	**Scan 0°**	**Scan 30°**	**Scan 60°**
1.70 GHz	44.46	43.79	41.14
1.75 GHz	44.65	43.97	41.61
1.80 GHz	44.73	44.13	41.39

Table 1. Directivity versus frequency per scan angle.